Human and Porcine Lumbar Endplate Injury Risk in Repeated Flexion-compression

Concetta F. Morino, Allison L. Schmidt, Elizabeth Dimbath, Shea T. Middleton, Jason R. Kait, Jay Shridharani, Maria A. Ortiz-Paparoni, Josh Klinger, Joost Op 't Eynde, Cameron R. 'Dale' Bass

Abstract Chronic low back pain (LBP) affects 50–80% of adults in their lifetimes, yet the injury etiology is unknown. Those exposed to repeated flexion-compression are at a higher risk for LBP, such as helicopter pilots and motor vehicle operators. Live animal lumbar injury models offer insight into *in vivo* injury mechanisms, but interspecies scaling is needed to relate live animal results to human. Human (n=16) and porcine (n=16) lumbar functional spinal units (FSUs) were loaded in repeated flexion-compression to establish endplate fracture risk. Applied flexion oscillated from 0 to 6° and applied peak stress ranged from 0.65 to 2.38 MPa for human and 0.64 to 4.68 MPa for porcine specimens. Six human and nine porcine specimens experienced endplate fracture. The 95% confidence intervals for human and porcine 50% injury risk curves in terms of stress and cycles overlapped, but the mean porcine injury risk was lower for a given stress level than that for human. An optimised constant stress scale factor of 0.742 on the 50% porcine risk results in a risk curve similar in shape and injury tolerance to human 50% risk. Further studies are needed to establish injury thresholds for tissue failure that may occur before endplate fracture.

Keywords Chronic back pain, combined loading, vertebral body endplate fracture, long duration loading, translating animal models to human.

I. INTRODUCTION

Low back pain (LBP) is one of the most prevalent conditions globally, currently affecting 28.6% of adults [1] and estimated to affect 50–80% of adults at some point in their lifetime [2]. LBP is a particular problem within the military. Back injury is the most commonly reported musculoskeletal injury, with lumbar injury specifically accounting for 20% of all reported musculoskeletal injuries among active-duty, non-deployed service members [3]. However, the etiology of LBP is not yet understood, with 90% of all LBP patients categorised with non-specific LBP, meaning no particular pathology can be confirmed [4]. Recent epidemiology studies have shown a higher prevalence of LBP for those with certain occupational activities, such as heavy lifting [2,5], bending [2,5], or those exposed to whole-body vibration such as helicopter pilots [6-8] and motor vehicle operators [9]. These occupational exposures are associated with flexion and repeated compression, which have both been shown to be contributing factors to lumbar injury [6,10-16]. To elucidate the factors that contribute to this widespread LBP, repeated combined flexion-compression needs to be studied under long-durations to understand injury risk that contributes to chronic LBP.

Several studies suggest many cases of LBP may originate from fracture or injury to the lumbar vertebral endplate. Vertebral endplates and outer annulus disc fibers are innervated, and therefore, major damage to these areas likely causes pain. It is possible that even minor damage to the endplate tissue may also result in pain[17]. Recent *in vitro* findings have shown the presence of endplate lesions to be significantly associated with those suffering from frequent LBP [18]. Hsu et al. found a significant increase in pain frequency when endplate fracture was detected for subjects imaged with discography compared to those imaged without detectable endplate damage[19]. For patients with lumbar endplate fractures that were treated surgically, LBP was significantly reduced or disappears completely, further supporting the hypothesis that endplate fracture is a contributing

C. M. Morino (e-mail: concetta.morino@duke.edu; tel: 919-660-5450) is a PhD candidate in Mechanical Engineering, A. L. Schmidt is a PhD graduate in Biomedical Engineering, E. Dimbath is a PhD student in Biomedical Engineering, S. T. Middleton is a PhD student in Biomedical Engineering, J. R. Kait is a Research Engineer in Biomedical Engineering, J. K. Shridharani is a PhD graduate in Biomedical Engineering, M. A. Ortiz-Paparoni is a Postdoctoral Associate in Biomedical Engineering, J. Klinger is an undergraduate student in Mechanical and Biomedical Engineering, J. Op 't Eynde is a PhD candidate in Biomedical Engineering, and C. R. Bass is an Associate Research Professor in Biomedical Engineering, all at Duke University in Durham, NC, USA.

factor of LBP in many patients [17]. Resolutions associated with current clinical radiographic diagnostic tools would not detect small endplate fractures or lesions, so associating this type of endplate injury with pain in clinical settings may be difficult and in most cases, unlikely [20,21].

To characterise LBP, it is essential to understand the cascade of biomechanical responses of the human lumbar spine *in vivo* leading up to the injury that may be associated with pain. While we can retrospectively study LBP through epidemiology, we cannot directly assess these human injury mechanisms *in vivo*. Cadaver human specimens are commonly used to study the injury behaviour within the osteoligamentous components of the spine (i.e. vertebral bodies, endplates, intervertebral discs, spinal ligaments) [22,23]. However, systems requiring physiology, such as the surrounding musculature and nervous tissue response can only be effectively studied *in vivo.*

The pig lumbar spine has been successfully used to model various behaviours in the human lumbar spine [24,25]. Thus, studying injury in a live pig model can directly assess physiological mechanisms of injury. However, while the pig lumbar spine can be a useful model for human lumbar due to the general similarities in anatomy [22], conclusions cannot be drawn about human lumbar injury behavior *in vivo* without interspecies scaling. To address this, the risk of lumbar injury due to repeated flexion-compression needs to be determined and compared *in vitro* for both the human and the porcine lumbar spine. This direct comparison can inform future live pig injury models and has the potential to elucidate human low back injury pain *in vivo* by further characterising the *in vitro* correlations between porcine and human spine.

II. METHODS

Experimental Testing

Cadaveric human (n=16) and porcine (n=16) lumbar functional spinal units (FSUs) were loaded in combined cyclic flexion-compression to establish the injury risk of endplate fracture due to long-term flexion-compression exposure. Human cadaver testing for this project was declared exempt by the Duke University Institutional Review board, and cadaveric porcine tissue was procured from post-mortem specimens of the Duke Division of Laboratory Animal Resources. Human donors were all male, aged 24–47 years. Porcine specimens were obtained from young adult Yorkshire pigs with an average mass of 65 kg. Specific human donor ages and pig weights for each test can be found in the Appendix (Table A.1). FSUs consisted of two adjacent vertebral bodies and their shared intervertebral disc (IVD). Most overlaying musculature was removed for vertebral body and IVD visibility, but some soft muscular tissue was left intact to preserve hydration. The osteoligamentous components were left intact. To fix the superior and inferior ends of the specimen to the aluminum cups attached to the mechanical testing system, two to four screws were inserted into the superior end of the superior vertebral body and the inferior end of the inferior vertebral body. Two 0.078” stainless steel wires were inserted into each vertebral body, 1-2 inches from the endplate, and bent for distal control of the vertebral body and to distribute stress. Wire and screws were then covered by polymethyl methacrylate (PMMA), and finally cast into aluminum cups with urethane casting resin (R1 Fast Cast® #891, Goldenwest Mfg, Inc., Grass Valley, CA). All specimens were imaged on a high-resolution (50–100 µm voxel size) x-ray computed tomography scanner (Nikon XTH 225 ST, microCT) prior to testing to screen for pre-existing degeneration and structural anomalies.

Specimens were rigidly secured to a biaxial mechanical testing system, equipped with two servohydraulic materials testing systems (MTS, Eden Prairie, MN, USA), inspired by the flexion-compression loading fixture from Callaghan et al. [26]. The fixture consisted of an axial actuator applying cyclic compression under axial force control and an independent rotational actuator applying cyclic flexion under angular displacement control (Fig. 1). Two 6-axis load cells (superior AMTI MC5-6-500 and inferior Denton 1716A) recorded the axial forces, anterior/posterior forces, and bending moments. A linear variable differential transformer (LVDT) measured linear displacements and an internal rotary variable differential transformer (RVDT) collected angular displacement. Data were sampled at 2 kHz. The superior end of the specimen was fixed to the rotational actuator while the inferior end was free to move in the left/right and anterior/posterior directions. This configuration allows for the center of rotation to move within the specimen and for the specimen to avoid large shear stresses that may not be representative of *in vivo* response for this type of loading. An environmental chamber surrounded the setup to maintain physiological *in vivo* temperature and humidity throughout testing (37°C and ~100% humidity). Acoustic sensors (Mistras S9225, Physical Acoustic Corporation, 300–1800 KHz) and hydrophones (Reson TC4013) were secured to the specimen for improved injury detection. Local areas were denuded of tissue down to the bone surface, and four acoustic sensors were glued to the specimen using cyanoacrylate glue, two

on each of the two vertebral bodies. Two hydrophones were secured to the soft tissue on the left and right side of the specimen. Figure A.1 in the Appendix shows how sensors were fixed to each test specimen.

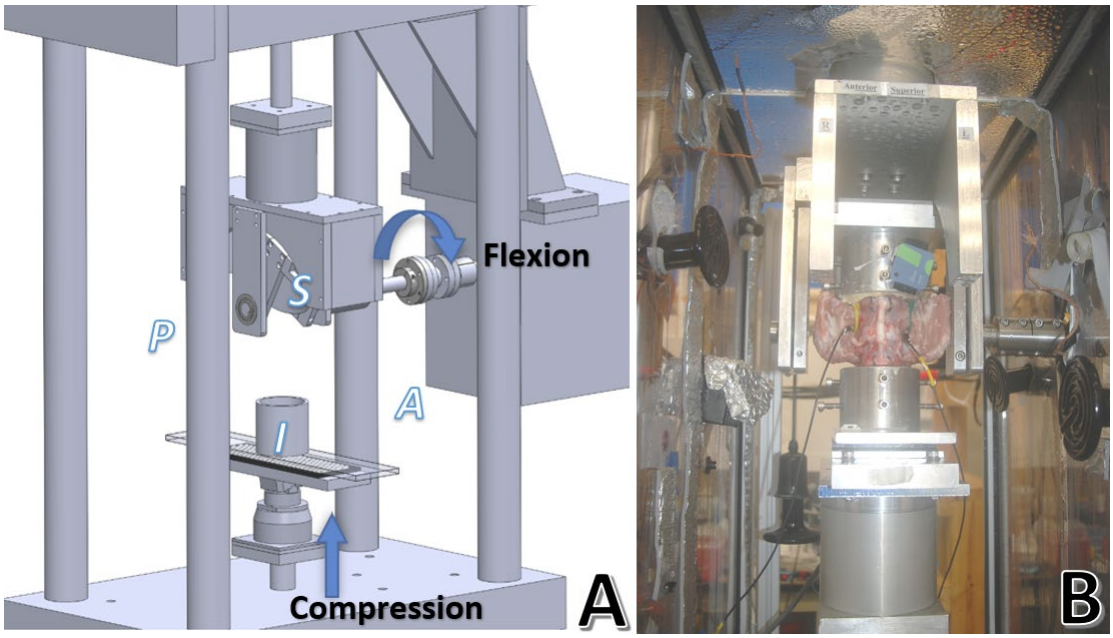

Fig. 1. (A) Schematic of flexion-compression combined loading biaxial test fixture. S/I signifies superior/inferior and A/P signifies anterior/posterior. Flexion is applied using the rotational actuator and axial compression is applied using the axial piston. (B) Anterior view of porcine FSU enclosed in environmental chamber.

The applied combined loading profile simulated real-world flexion and compression exposure for seated occupants in high-speed watercraft [27] (Fig. 2). Sinusoidal compression was applied under force control at 1 Hz from a minimum compressive load to a prescribed peak compressive load, simulating the repeated vertical compression experienced by seated occupants. An offset flexion wave was independently applied under displacement control with a ramp starting at 80% of the compressive peak from 0° to 6° for all tests. This applied flexion profile simulates the resulting lumbar flexion response to seated occupants influenced by the repeated predominantly vertical impacts and upper body inertia.

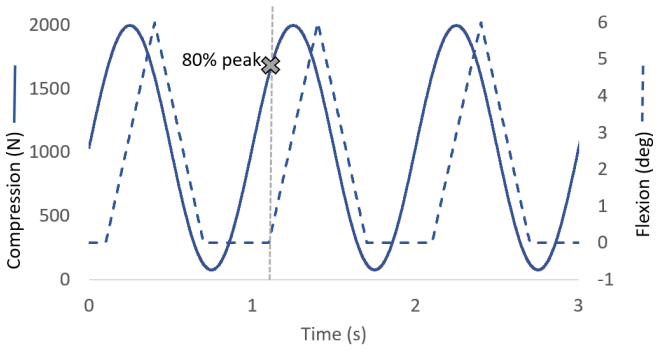

Fig. 2. Applied compression (solid) and flexion (dashed) for a porcine fatigue test. Compression was applied as a sinusoid at 1 Hz. Flexion was applied as a ramp, starting at 80% of the compressive peak.

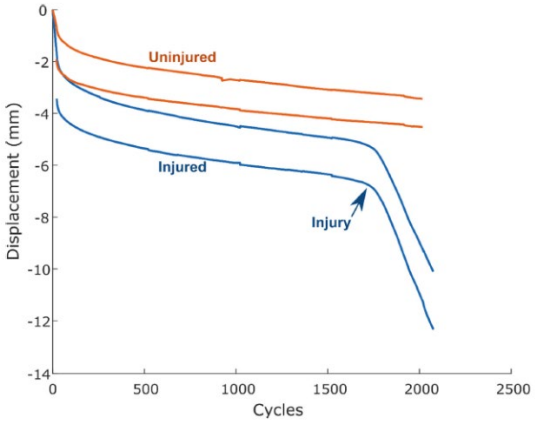

Fig. 3. The orange lines show the minimum and maximum displacement response of the oscillatory profile from a non-injury human test. The blue lines from an injury test show a clear inflection in the creep profile, signifying a change in the load-bearing capacity of the specimen [28].

The human test series was performed first. Loading parameters for subsequent porcine tests were informed by the human test series. Average endplate (EP) areas, minimum loads, applied force range and applied stress range for each test series can be found in Table I. The minimum load for all human tests was chosen to be 200 N. The lumbar supports roughly 40% of the body's mass[29]. This value of 200 N was chosen to represent a minimum

compression on the human lumbar spine without external load, which was approximately 40% body mass minus a nonzero abdominal muscle contribution. To develop an injury risk for a wide range of loading exposures that required more than one cycle to fail, prescribed peak compressive loads ranged from 1000 N and 3000 N in human tests, below the ultimate compressive strength for human lumbar vertebral body[30]. The minimum load for all porcine tests was chosen by scaling the minimum human load of 200 N by endplate area, which was measured to be approximately 2.63x smaller in the initial porcine specimens. Informed by this endplate ratio, 76 N was chosen for the minimum porcine compression, applied to all porcine tests for consistency. Prescribed peak loads for the porcine test series ranged from 300 N to 2300 N, initially informed by stress values associated with human endplate fracture results, and later informed by early porcine tests failure results. Four endplate cross-sectional area measurements were taken for each FSU using pre-test microCT transverse images and averaged (one measurement for each endplate of the four endplates in one FSU). After loading, specimens were imaged again with the high-resolution microCT to determine assess potential fractures.

TABLE I
HUMAN AND PORCINE TEST SERIES INFORMATION

Test Series	*Spinal Level Range*	*Average EP Area (cm^2)*	*Minimum Load (N)*	*Applied Peak Load (N)*	*Applied Stress (MPa)*
Human	T12–S1	16.68	200	1000–3000	0.65–2.38
Pig	T15–L6	5.52	76	300–2300	0.64–4.68

Accelerated Life Analysis

An accelerated life analysis was performed for both the human and pig datasets independently using MiniTab v20.4 (Minitab Inc. State College, PA, USA). Because human chronic lumbar injury risk occurs on a timescale of seconds to years, accelerated life analysis is used to assess risk over shorter periods that are amenable to testing. Accelerated life analysis is similar to survival analysis, informed by fatigue tests under higher loads and shorter durations to predict failure under lower loads and longer durations, such as the real-world occupational loading exposures mentioned earlier. For this reason, this analysis is particularly useful for biomechanical failure testing in biological tissues and tissue surrogates[31-33].

Applied compressive force was initially used for the accelerating variable, and then the analysis was performed again using applied stress as the accelerated variable. A parametric Weibull distribution was chosen for both porcine and human datasets. Injury/failure was defined as endplate fracture and was confirmed on the post-test high-resolution microCT. Non-injury data points were right censored. Injury points were interval censored from 0 cycles to the cycle after the inflection in the displacement trace. Figure 3 shows an example displacement trace from both a noninjury and injury test. The inflection shown in the displacement response for the injured specimen shows a significant change in the structural integrity of the spinal unit. All injured specimens that showed this displacement characteristic resulted in an endplate failure. Therefore, this displacement data was utilised to inform the interval bounds.

III. RESULTS

Six of 16 human specimens and nine of 16 porcine specimens experienced endplate fractures, all confirmed by post-test high-resolution microCT imaging (Fig. 4). Total test times ranged from four minutes to six days in the human test series, with the longest test resulting in a non-injury point. Total test times for the porcine series ranged from 7 minutes to 80 hours (>3 days). Time to injury for injured specimens and total test time for uninjured specimens are shown in Fig. 5, along with censoring direction denoted by the associated arrows. Endplate and vertebral body injuries for each test can be found in the Appendix (Table A.1). Note that the specific loading duration after incipient endplate failure cannot be definitively determined and widely varies for each test. Therefore, no conclusions can necessarily be made about the association between injury severity and loading conditions.

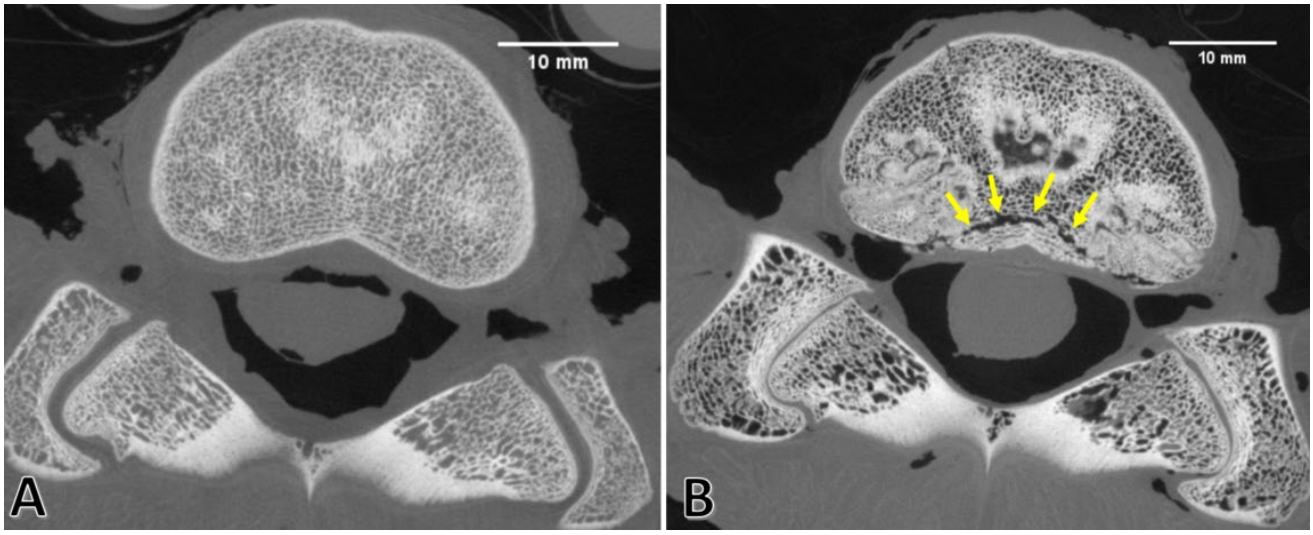

Fig. 4. (A) High-resolution (86.8 µm/pixel) microCT transverse image of porcine vertebral body endplate prior to testing. (B) After loading, endplate fracture (yellow arrows) resulting after long duration flexion-compression.

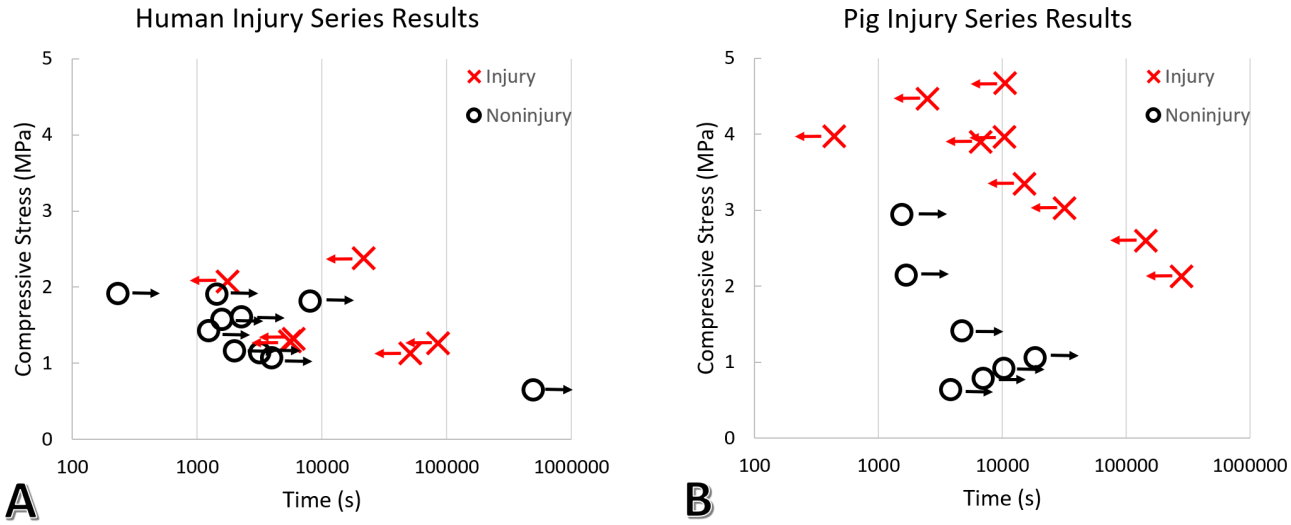

Fig. 5. Injury and non-injury results from human (A) and pig (B) test series. Right-facing arrows with non-injury points symbolise right censoring. Left-facing arrows with injury points symbolise interval censored data points, bound from 0 to after the displacement inflection.

The 50% endplate fracture injury risks for both the human and pig test series are shown in Fig. 6, along with the 95% confidence intervals denoted by the dashed lines. Figure 6A shows the injury risk in terms of applied compressive force and cycles, while Figure 6B shows injury risk in terms of compressive stress and cycles. The 50th percentile risk represents a 50% risk that a human (or pig) would experience a lumbar endplate fracture at a particular force and cycle count if continuously loaded in flexion and compression at 1 Hz. Because loading was applied at 1 Hz, loading duration in seconds and cycle count are equivalent here. The overall log-time slope for the porcine risk function is similar to that of the human series when assessing risk in terms of stress. There is a large difference in size between the two species so with size difference considerations and considering that the injury risk profiles show greater similarity in risk behaviour when assessed in terms of stress, the rest of the analysis will focus on injury risk using stress. Equations 1 and 2 show the equations for the 50% injury risk for human and pig series based on applied stress, respectively.

Whole the confidence intervals overlap between the two species, the porcine 50% injury risk shows larger fracture tolerance for the same stress compared to that of the human series. There was no information beyond 2.38 MPa to inform the human series risk, unlike the porcine series, which included specimens experiencing up to 4.68 MPa in applied compressive stress.

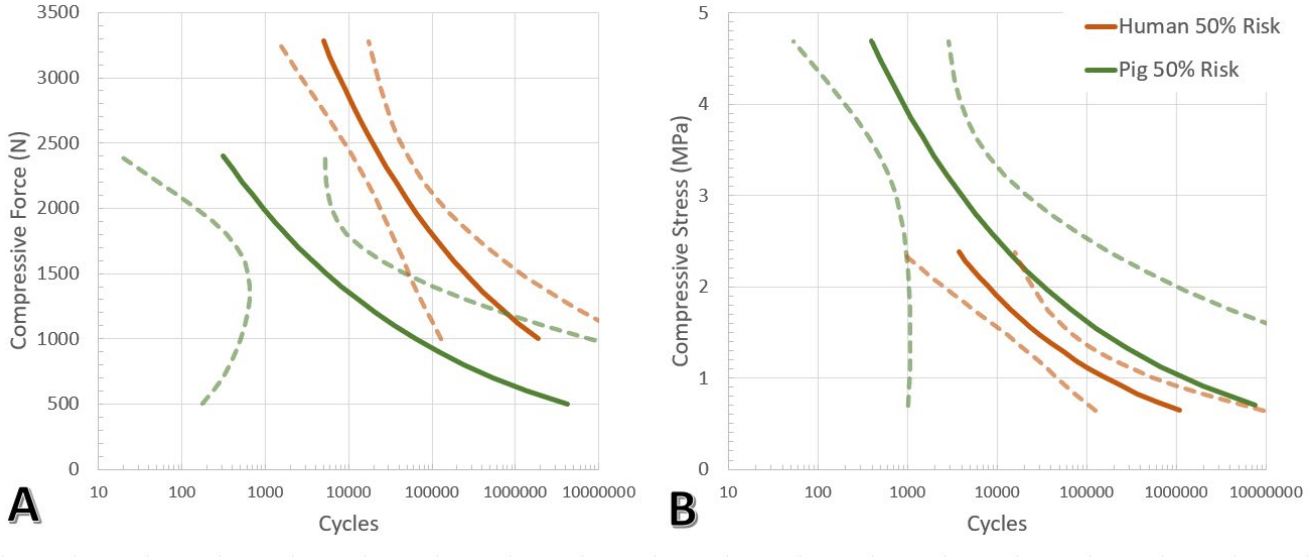

Fig. 6. Human vs. porcine endplate fracture 50th percentile injury risks (solid lines) with 95% confidence intervals (dashed lines) in terms of cycle count and (A) compressive force (B) compressive stress.

$$\sigma_{human}(MPa) = 15.66e^{-0.528 \cdot \log(cycles)} \quad (1)$$

$$\sigma_{pig}(MPa) = 14.81e^{-0.443 \cdot \log(cycles)} \quad (2)$$

IV. Discussion

The resulting injury risk curves show the 50th percentile risks for endplate fracture in both the human and pig when exposed to repeated flexion-compression in terms of stress and loading duration. The 95% confidence intervals of the two risk curves overlap and the two slopes' dependence on cycles to failure for a given force are similar, which shows that the two species are comparable for injury in this loading configuration. However, while the risk for human and pig are similar, for a given applied stress, the predicted cycles to failure in the pig are much greater than for that of the human lumbar spine. For example, at 2 MPa of applied compressive stress, the 50% human risk occurs at approximately 7900 s (or 2.2 hours) and the 50% pig risk occurs at approximately 33,100 s (or 9.2 hours).

The resulting injury risk curves for the two species can be used together to translate pig endplate injury results to human in terms of stress. If the pig experiences endplate injury for 1.4 MPa of applied stress at 211,000 s, then the equivalent 50% human injury risk shows that the human could only tolerate 0.94 MPa for the same loading duration. The other interpretation would be that for 1.4 MPa of applied stress, the human lumbar spine would only tolerate less than 38,000 s of loading before fracture. This injury translation would be particularly useful when interpreting injury in *in vivo* porcine models.

However, if we consider scaling the 50% porcine injury risk to human injury risk using a constant scale factor, the difference between the two curves becomes much smaller. A constant scale factor of 0.742 was found by optimising this coefficient to minimise the sum of squared error between the two curves. The resulting scaled pig 50% risk lies almost directly on top of the human 50% risk (Fig. 7). The updated scaled pig equation is shown in Equation 3. With the application of this additional scale factor, the sum of squared errors between the human and pig 50% risk curves decreased by 98%. Using this additional scale factor applied to the porcine stress-based risk equation provides a direct translation between the two species' injury risk.

$$\sigma_{pig_{scaled}}(MPa) = 10.99e^{-0.443 \cdot \log(cycles)} \quad (3)$$

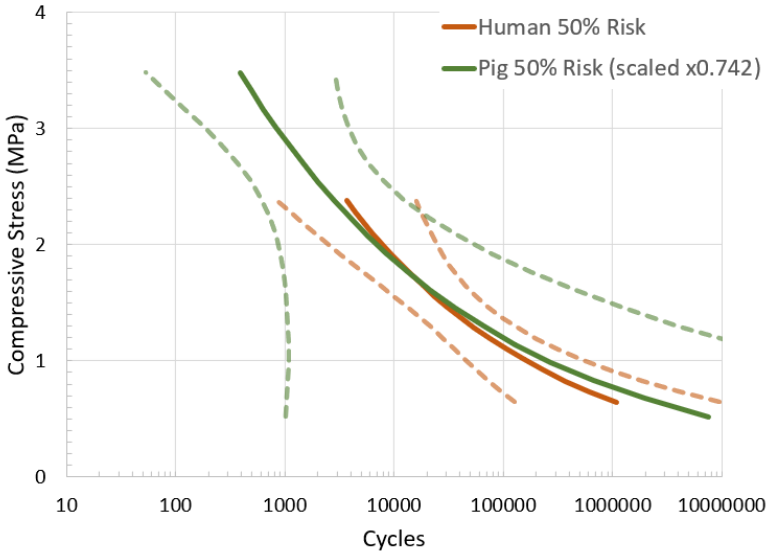

Fig. 7. Endplate 50% injury risk in terms of compressive stress and cycle count for human (red) and scaled porcine (green) 95% confidence intervals (dashed lines).

The results imply that for a given stress, the porcine lumbar can tolerate longer loading durations before endplate failure when compared to human lumbar. The 0.742 scale factor applied to the pig 50% risk translates the pig risk to be very similar to the human risk. The exact interspecies differences driving this additional scale factor for endplate fracture risk is unknown.

Many studies have documented the various anatomical differences between human and porcine lumbar vertebrae such as significant differences in vertebral body height [34], endplate depth and width [34], and IVD geometry [35] that may play a role in load distribution. This difference in endplate fracture tolerance may be largely influenced by documented material differences between human and pig vertebral bodies and endplates. Aerssens et al. found the porcine trabecular bone in the lumbar vertebrae to have significantly greater bone mineral density and bone mineral content than that of human lumbar vertebrae [36]. When directly comparing lumbar endplate differences, while the human endplates are significantly thicker, the porcine endplates have significantly higher cellular density throughout [37]. There also exist notable differences in collagen fiber organization between the human and porcine endplate with human central endplates containing neat, parallel fiber alignment, while the porcine central endplate collagen fibers were intertwined, which may influence load bearing capacity [37]. Regarding the IVD properties for each species, porcine discs have been shown to be stiffer than that of the human with a significantly reduced normalized range of motion [35]. It is possible that any or all of these material differences collectively influence the porcine endplate to be mechanically tougher than the human lumbar endplate under the same stress conditions. Further, the age of the pig may greatly influence endplate toughness in this test series. The pigs used in this study were young adult pigs, but the variation of endplate toughness just within the porcine population may be large with how quickly pigs mature physically. Meanwhile, the human population varied from 24 to 47 years of age. IVD degeneration that commonly exists in the middle-aged human population likely does not exist in the young adult porcine population used in this study. While no pre-existing injuries or abnormalities were detected prior to testing and this human population was relatively young, the human specimens experienced decades of loading pre-mortem, unlike the porcine population. Any minor degeneration in the human population could affect the load-bearing capacity of the FSU and therefore, result in earlier failure in the human endplates for the same applied stress level.

Differences in injury tolerance may also be explained by strain differences. The current failure points do not account for axial strains experienced by each specimen. It is possible that the resulting strains experienced by the human specimens differ greatly from the strains experienced by the porcine specimens. In porcine tests, maximum displacements for some failure tests extended beyond the measured height of the IVD, implying other tissues, such as the endplates, were experiencing substantial strains. Additional displacement beyond the IVD height could have exposed the endplates to a greater stress than calculated. Further investigation should be carried out to understand the source of this currently unknown interspecies scaling factor. Regardless of the driving factors influencing the difference in fracture tolerance, the established injury risks and scaled injury risks

provide an interspecies risk translation that can be used in future studies involving lumbar injury for both humans and pigs.

The effect of water loss from the discs is important for loading in this time scale. As previously noted, these specimens were continuously loaded with no recovery periods. Even though the specimens were loaded in a saturated humidity chamber, specimens lost a considerable amount of water in the discs throughout the loading period, particularly for those specimens loaded on the magnitude of days. This water loss is evident in the post-test image compared the pre-test imaging of the three-day porcine test (Fig. 4). Between the trabeculae cavities, pre-test imaging shows densities consistent with water that appear black in post-test images. This water loss is not necessarily a consequence of *in vitro* loading but a result of mechanical fluid flow that also occurs *in vivo* due to diurnal loading [38,39]. The mechanical pressure due to diurnal loading forces water out of the disc, which is restored through passive diffusion during long rest periods when external load is relieved [39-41]. Water content is crucial for both the physiological and mechanical function of the disc [42-44]. Long recovery periods on the scale of 3–4x that of the loading period are necessary to restore water content and restore mechanical function [41,45]. So, the presence of recovery periods would likely increase injury tolerance. Educated estimations can be made from these injury risk results to predict injury tolerance from cyclic flexion-compression loading on the timescale of months to years with regular physiological rest periods.

There are several limitations in this study. Acoustic emissions were initially intended to be used to determine specific time-to-fracture conditions and narrow the censoring interval. However, the results from the acoustic emissions were not consistent throughout the pig and human test series, with only a few failure tests producing detectable acoustic emissions. Therefore, failure data in this study was censored with much wider intervals than expected had the resulting acoustic data been more accurate and consistent. Further, this injury risk determination was established specifically for endplate failure. Endplate failure is easily determined from imaging tools and is typically associated with a clear change in load-bearing capacity shown in the displacement response. However, endplate fracture is likely not the first failure caused by combined flexion-compression loading. Rather, endplate failure is likely the result of a significant compromise in the structural integrity of the intervertebral disc. In every failed specimen, the IVD was severely disrupted in both the annulus fibrosus fibers and nucleus pulposus. Additionally, many ‘uninjured’ specimens without endplate fracture showed signs of disc failure, indicating that this type of tissue failure may precede endplate failure. The authors intend to utilise this dataset with additional testing to determine the injury risks for disc failures. Current clinical imaging modalities are not yet capable of resolving the microscopic disruptions to the disc *in vivo* that may be contributing significantly to chronic pain. By narrowing the injury risk closer to incipient injury on the µm scale, resulting injury risk analyses could inform risk predictions, particularly for those regularly exposed to these cyclic loads.

Finally, there were limitations due to *in vitro* experimentation. First, the mechanical roles of relevant physiology in the lumbar region, such as musculature, tendons, and abdominal pressure, are unknown along with how they influence the injury risk *in vivo*. Similar loading patterns need to be investigated in live animal models to properly study these effects. *In vitro* injury results cannot directly be associated with pain. Endplate failure likely causes pain, as shown in previous work [17-19], but chronic pain may be associated with lower-level soft tissue injury occurring prior to endplate failure. Without live animal tests, this study cannot directly address the onset, intensity, or progression of pain symptoms.

This fatigue investigation was unique such that human and pig specimens were exposed to combined flexion-compression for multiple days. No other studies into lumbar fatigue due to this repeated loading exist on this time scale. By applying greater loads than what may be experienced in diurnal loading, an accelerated life analysis provides an educated prediction into injury risk for loads closer to realistic occupational loads. The prescribed loading for these tests was at a frequency of 1 Hz, so the loading duration was equivalent to the cycle count. However, with lower frequencies, i.e. impacts occurring every 5 s, 100 cycles might be interpreted as a loading duration of 500 s. Though, due to viscoelastic considerations, this is notably a simplified approximation. Further, loading was applied constantly without recovery. Therefore, these long-duration injury risk predictions can be used to guide injury risk predictions for loading exposures on the magnitude of months to years when periodic rest is accounted for.

V. CONCLUSIONS

This study is the first to establish injury risk criteria for the human and porcine lumbar spine loaded in combined flexion-compression for long durations, elucidating the injury risk for loads similar to occupational exposures in several professions, including high-speed watercraft. By applying the similar loading configuration and conditions to two species over a range of applied forces, this study presents an extremely useful direct comparison between a commonly used animal model and human for this combined loading type. The two injury risk curves showed comparable injury risk in terms of stress and cycles, but the 50% risk curves indicate that the porcine specimens tolerate longer loading durations for the same applied stress when compared to human. While the biomechanics accounting for these differences in injury tolerance between the two species are not currently known, applying an additional optimised stress scaling factor of 0.742 to porcine risk model creates a ~1:1 translation between the 50% porcine and human risks. The resulting scaled injury risks can be used to translate risk from pig to human for flexion-compression loading in future *in vitro* and *in vivo* tests, leading to a better understanding of lumbar injury and lumbar pain for *in vivo* human. Endplate injuries produced in this study may be associated with chronic pain that may be overlooked clinically, due to relatively low-resolution diagnostic tools currently available. Further investigation is required to establish lower-level soft tissue injury risk that may be occurring prior to endplate failure.

VI. ACKNOWLEDGEMENTS

The authors gratefully acknowledge funding from the Office of Naval Research and US Naval Air Systems Command – Patuxent River through MTEC (Southwest Research Institute-PI).

VII. REFERENCES

[1] Lo, J., Chan, L., and Flynn, S. A systematic review of the incidence, prevalence, costs, and activity and work limitations of amputation, osteoarthritis, rheumatoid arthritis, back pain, multiple sclerosis, spinal cord injury, stroke, and traumatic brain injury in the United States: a 2019 update. *Archives of physical medicine and rehabilitation*, 2021. 102(1): p. 115-131

[2] Fatoye, F., Gebrye, T., and Odeyemi, I. Real-world incidence and prevalence of low back pain using routinely collected data. *Rheumatology international*, 2019. 39(4): p. 619-626

[3] Hauret, K.G., Jones, B.H., Bullock, S.H., Canham-Chervak, M., and Canada, S. Musculoskeletal injuries: description of an under-recognized injury problem among military personnel. *American journal of preventive medicine*, 2010. 38(1): p. S61-S70

[4] Maher, C., Underwood, M., and Buchbinder, R. Non-specific low back pain. *The Lancet*, 2017. 389(10070): p. 736-747

[5] Rubin, D.I. Epidemiology and risk factors for spine pain. *Neurologic clinics*, 2007. 25(2): p. 353-371

[6] De Oliveira, C.G. and Nadal, J. Transmissibility of helicopter vibration in the spines of pilots in flight. *Aviation, space, and environmental medicine*, 2005. 76(6): p. 576-580

[7] Knox, J.B., Deal, J.B., and Knox, J.A. Lumbar disc herniation in military helicopter pilots vs. matched controls. *Aerospace medicine and human performance*, 2018. 89(5): p. 442-445

[8] Byeon, J.H., Kim, J.W., et al. Degenerative changes of spine in helicopter pilots. *Annals of rehabilitation medicine*, 2013. 37(5): p. 706

[9] Knox, J.B., Orchowski, J.R., et al. Occupational driving as a risk factor for low back pain in active-duty military service members. *The Spine Journal*, 2014. 14(4): p. 592-597

[10] Gallagher, S., Marras, W.S., Litsky, A.S., and Burr, D. Torso flexion loads and the fatigue failure of human lumbosacral motion segments. *Spine*, 2005. 30(20): p. 2265-2273

[11] Desmoulin, G.T., Pradhan, V., and Milner, T.E. Mechanical aspects of intervertebral disc injury and implications on biomechanics. *Spine*, 2020. 45(8): p. E457-E464

[12] Thoreson, O., Ekström, L., et al. The effect of repetitive flexion and extension fatigue loading on the young porcine lumbar spine, a feasibility study of MRI and histological analyses. *Journal of experimental orthopaedics*, 2017. 4: p. 1-9

[13] Wade, K.R., Robertson, P.A., Thambyah, A., and Broom, N.D. How healthy discs herniate: a biomechanical and microstructural study investigating the combined effects of compression rate and flexion. *Spine*, 2014. 39(13): p. 1018-1028

[14] Schmidt, A.L., Paskoff, G., Shender, B.S., and Bass, C.R. Risk of lumbar spine injury from cyclic compressive loading. *Spine*, 2012. 37(26): p. E1614-E1621

[15] Hansson, T., Keller, T., and Spengler, D. Mechanical behavior of the human lumbar spine. II. Fatigue strength during dynamic compressive loading. *Journal of Orthopaedic Research*, 1987. 5(4): p. 479-487

[16] Tsai, K., Lin, R., and Chang, G. Rate-related fatigue injury of vertebral disc under axial cyclic loading in a porcine body-disc-body unit. *Clinical Biomechanics*, 1998. 13(1): p. S32-S39
[17] Peng, B., Chen, J., et al. Diagnosis and surgical treatment of back pain originating from endplate. *European Spine Journal*, 2009. 18: p. 1035-1040
[18] Wang, Y., Videman, T., and Battié, M.C. ISSLS prize winner: lumbar vertebral endplate lesions: associations with disc degeneration and back pain history. *Spine*, 2012. 37(17): p. 1490-1496
[19] HSU, K.Y., ZUCHERMAN, J.F., et al. Painful lumbar end-plate disruptions: a significant discographic finding. *Spine*, 1988. 13(1): p. 76-78
[20] Lotz, J., Fields, A., and Liebenberg, E. The role of the vertebral end plate in low back pain. *Global spine journal*, 2013. 3(3): p. 153-163
[21] Van Dieën, J., Weinans, H., and Toussaint, H. Fractures of the lumbar vertebral endplate in the etiology of low back pain: a hypothesis on the causative role of spinal compression in aspecific low back pain. *Medical hypotheses*, 1999. 53(3): p. 246-252
[22] Busscher, I., van der Veen, A.J., et al. In vitro biomechanical characteristics of the spine: a comparison between human and porcine spinal segments. *Spine*, 2010. 35(2): p. E35-E42
[23] Ortiz-Paparoni, M., Op 't Eynde, J., et al. The Human Lumbar Spine During High-Rate Under Seat Loading: A Combined Metric Injury Criteria. *Ann Biomed Eng*, 2021. 49(11): p. 3018-3030
[24] Bass, C.R., Rafaels, K.A., et al. Thoracic and lumbar spinal impact tolerance. *Accid Anal Prev*, 2008. 40(2): p. 487-95
[25] Araújo, A., Peixinho, N., Pinho, A., and Claro, J.C.P. Comparison between the dynamic and initial creep response of porcine and human lumbar intervertebral discs. *Proceedings of 2015 IEEE 4th Portuguese Meeting on Bioengineering (ENBENG)*, 2015.
[26] Callaghan, J.P. and McGill, S.M. Intervertebral disc herniation: studies on a porcine model exposed to highly repetitive flexion/extension motion with compressive force. *Clinical Biomechanics*, 2001. 16(1): p. 28-37
[27] Bass, C.R., Salzar, R., Ziemba, Z., Lucas, S., and Peterson, R. The modeling and measurement of humans in high speed planing boats under repeated vertical impacts. *Proceedings of International Research Conference on the Biomechanics of Impact (IRCOBI)*, 2005.
[28] Schmidt, A.L. Assessing the Injury Tolerance of the Human Spine. 2017, Duke University.
[29] Plagenhoef, S., Evans, F.G., and Abdelnour, T. Anatomical data for analyzing human motion. *Research quarterly for exercise and sport*, 1983. 54(2): p. 169-178
[30] Brinckmann, P., Biggemann, M., and Hilweg, D. Fatigue fracture of human lumbar vertebrae. *Clinical biomechanics*, 1988. 3: p. i-S23
[31] Wells, S.M., Sellaro, T., and Sacks, M.S. Cyclic loading response of bioprosthetic heart valves: effects of fixation stress state on the collagen fiber architecture. *Biomaterials*, 2005. 26(15): p. 2611-2619
[32] Sacks, M.S. and Smith, D.B. Effects of accelerated testing on porcine bioprosthetic heart valve fiber architecture. *Biomaterials*, 1998. 19(11-12): p. 1027-1036
[33] Wenz, L., Brown, S., Moet, A., Merritt, K., and Steffee, A. Accelerated testing of a composite spine plate. *Composites*, 1989. 20(6): p. 569-574
[34] Dath, R., Ebinesan, A., Porter, K., and Miles, A. Anatomical measurements of porcine lumbar vertebrae. *Clinical biomechanics*, 2007. 22(5): p. 607-613
[35] Beckstein, J.C., Sen, S., Schaer, T.P., Vresilovic, E.J., and Elliott, D.M. Comparison of animal discs used in disc research to human lumbar disc: axial compression mechanics and glycosaminoglycan content. *Spine*, 2008. 33(6): p. E166-E173
[36] Aerssens, J., Boonen, S., Lowet, G., and Dequeker, J. Interspecies differences in bone composition, density, and quality: potential implications for in vivo bone research. *Endocrinology*, 1998. 139(2): p. 663-670
[37] Li, Y.H., Wu, H.L., et al. Species variation in the cartilaginous endplate of the lumbar intervertebral disc. *JOR spine*, 2022. 5(3): p. e1218
[38] Van der Veen, A., Van Dieen, J., Nadort, A., Stam, B., and Smit, T. Intervertebral disc recovery after dynamic or static loading in vitro: is there a role for the endplate? *Journal of biomechanics*, 2007. 40(10): p. 2230-2235
[39] Bezci, S.E. and O'Connell, G.D. Osmotic pressure alters time-dependent recovery behavior of the intervertebral disc. *Spine*, 2018. 43(6): p. E334-E340
[40] Ayotte, D., Ito, K., and Tepic, S. Direction-dependent resistance to flow in the endplate of the intervertebral disc: an ex vivo study. *Journal of Orthopaedic Research*, 2001. 19(6): p. 1073-1077
[41] O'Connell, G.D., Jacobs, N.T., Sen, S., Vresilovic, E.J., and Elliott, D.M. Axial creep loading and unloaded recovery of the human intervertebral disc and the effect of degeneration. *Journal of the mechanical behavior of biomedical materials*, 2011. 4(7): p. 933-942
[42] Das, D.B., Welling, A., Urban, J., and Boubriak, O. Solute transport in intervertebral disc: experiments and finite element modeling. *Annals of the New York academy of sciences*, 2009. 1161(1): p. 44-61
[43] Adams, M.A. and Roughley, P.J. What is intervertebral disc degeneration, and what causes it? *Spine*, 2006. 31(18): p. 2151-2161

[44] Paul, C.P., Emanuel, K.S., et al. Changes in intervertebral disk mechanical behavior during early degeneration. *Journal of biomechanical engineering*, 2018. 140(9)

[45] Johannessen, W., Vresilovic, E.J., Wright, A.C., and Elliott, D.M. Intervertebral disc mechanics are restored following cyclic loading and unloaded recovery. *Annals of biomedical engineering*, 2004. 32: p. 70-76

VIII. APPENDIX

TABLE A.I
SPECIMEN INFORMATION AND ENDPLATE/VERTEBRAL BODY INJURY SUMMARY

Human	Test	Spinal Level	Average EP Area (cm^2)	Subject Age	Endplate (EP) and Vertebral Body (VB) Injury
	1	L3-L4	14.79	47	
	2	T12-L1	21.00	44	
	3	L2-L3	18.69	44	
	4	L4-L5	19.11	44	
	5	T12-L1	14.45	42	*L1*: Anterior EP Fx (multiple)
	6	L2-L3	15.74	42	
	7	L4-L5	17.60	42	
	8	T12-L1	15.16	40	*L1*: Depression / Stellate EP Fx
	9	L2-L3	17.24	40	
	10	L4-L5	18.66	40	
	11	L1-L2	16.52	24	
	12	L3-L4	17.62	24	*L4*: Stellate EP Fx (multiple)
	13	L5-S1	15.55	24	*S1*: Complete transverse Fx of Inferior VB, anterior EP fx
	14	T12-L1	12.63	35	*T12*: VB burst, multiple EP Fx *L1*: VB burst, multiple EP Fx
	15	L2-L3	15.78	35	*L2*: Stellate EP Fx
	16	L4-L5	15.50	35	
Pig	**Test**	**Spinal Level**	**Average EP Area (cm^2)**	**Pig Mass (kg)**	**Endplate (EP) and Vertebral Body (VB) Injury**
	1	L2-L3	4.81	41	*L3*: Anterior EP Fx
	2	L4-L5	5.08	41	*L4*: Multiple EP Fx *L5*: Multiple EP Fx, complete transverse Fx through L5
	3	L1-L2	5.29	64	*L2*: Anterior EP Fx
	4	L3-L4	5.84	64	*L3*: VB Fx in posterior, right, left, multiple EP Fx *L4*: Fx in EP/VB fusion, multiple EP Fx
	5	L5-L6	6.03	64	*L5*: Multiple EP Fx, VB burst *L6*: Anterior left VB Fx, posterior/central EP Fx
	6	T15-L1	5.92	69	*T15*: Multiple EP Fx (left, right) *L1*: Multiple EP Fx (posterior, left and right)
	7	L1-L2	4.48	38	*L1*: EP Fx on specimen right *L2*: Posterior EP Fx
	8	L3-L4	4.86	45	*L3*: EP Fx on specimen left
	9	L1-L2	4.60	45	
	10	L5-L6	7.07	88	
	11	L1-L2	7.49	88	
	12	L1-L2	6.15	86	
	13	L2-L3	7.05	84	
	14	L1-L2	5.84	73	
	15	L5-L6	6.57	86	*L6*: Multiple EP Fx (posterior, anterior left)
	16	L2-L3	5.94	70	*L2*: Large posterior EP Fx, EP Fx on specimen right *L3*: Anterior EP Fx through left to right, posterior EP Fx, multiple EP Fx (central)

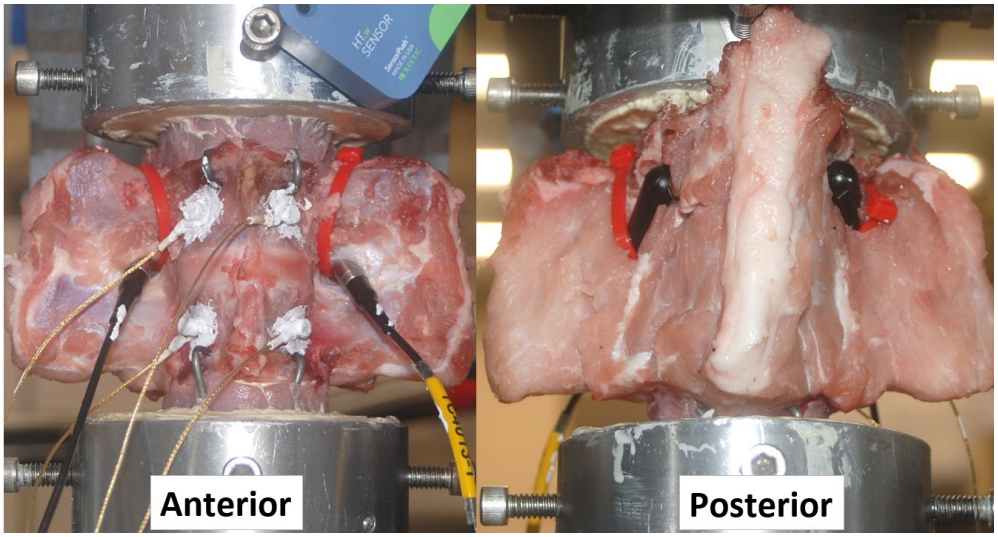

Figure A.1: Specimen instrumentation including four acoustic sensors attached to vertebral bodies and two hydrophones secured to posterior soft tissue. Major ligaments, such as the anterior longitudinal ligament, supraspinous ligament, and intertransverse ligaments were left intact.